Talón-Argente, E.; Lampi, A.; Vargas, M.; Chiralt, A.; Jouppila, K.; González Martínez, MC. (15-1). Encapsulation of eugenol by spray-drying using whey protein isolate or lecithin: Release kinetics, antioxidant and antimicrobial properties. Food Chemistry. 295:588-598. https://doi.org/10.1016/j.foodchem.2019.05.115

Encapsulation of eugenol by spray-drying using whey protein isolate or lecithin: Release kinetics, antioxidant and antimicrobial properties.

Emma Talón[1]*; Anna-Maija Lampi[2]; María Vargas[1]; Amparo Chiralt[1]; Kirsi Jouppila[2]; Chelo González-Martínez[1]

[1] *Instituto Universitario de Ingeniería de Alimentos para el Desarrollo, Universitat Politècnica de València, Spain.* *emtalar@etsid.upv.es

[2] *Department of Food and Environmental Sciences, University of Helsinki, Finland.*

Abstract

The encapsulation of eugenol (E) by spray-drying using whey protein (WP) or soy lecithin (LE) and maltodextrin in combination with oleic acid (OA) and chitosan (CH) was analysed in order to obtain antioxidant and antimicrobial powders for food applications. Formulations with only WP or LE showed higher encapsulation efficiencies (EE) (95-98%) and antibacterial effect against E. coli and L. innocua due to their greater E load. Incorporation of OA or CH promoted lower EE, which negatively affected the antimicrobial and antioxidant activities of the powders. Furthermore, the addition of CH implied less thermal protection against the E losses. The eugenol release was not notably affected by pH or polarity of the food simulant, but the release rate significantly decreased when incorporating OA and CH. The E-LE formulations better retained the eugenol than E-WP powders when heated above 200 ºC, this being relevant for the powder inclusion in thermally treated products.

Keywords: encapsulation efficiency, release kinetics, oleic acid, chitosan, antioxidant capacity, antibacterial properties.

1. Introduction

Over the last few years, substantial efforts have been focused on making use of natural compounds to develop novel health-promoting ingredients for use in the food industry. In this sense, increasing interest has been shown in the extracts from aromatic plants, such as essential oils, due to their antioxidant and antimicrobial properties (Prakash, Kedia, Mishra & Dubey, 2015). Eugenol (E) is a natural phenolic substance found as a major compound in different plant essential oils, such as clove, nutmeg, cinnamon or basil (Chatterjee & Bhattacharjee, 2013). Particular antimicrobial activity for E has been described by different authors against Gram positive and Gram negative bacteria (*Bacillus subtilis, Clostridium sporogenes, Enterococcus faecalis, Lactobacillus plantarum, Listeria monocytogenes, Escherichia coli* and *Salmonella pullorum,* (Dorman & Deans, 2000)), fungi (*Aspergillus carbonarius and Penicillium roqueforti* (Šimović, Delaš, Gradvol, Kocevski & Pavlović, 2014)) and yeast (*Saccharomyces cerevisiae* and *Candida* (Pinto, Vale-Silva, Cavaleiro & Salgueiro, 2009)). Its effective antioxidant capacity has also been studied by several authors (Kamatou, Vermaak & Viljoen, 2012; Ogata, Hoshi, Urano & Endo, 2000). Chatterjee & Bhattacharjee (2015) successfully incorporated eugenol-rich clove extract in mayonnaise as a flavoring agent and as a source of natural antioxidants to improve its shelf-life and functional value. Cortes-Rojas, Souzca & Oliveira (2014) also produced antioxidant powder products with solid lipid nanoparticles (SLN) containing eugenol.

Nevertheless, the beneficial properties of eugenol can be reduced by inadequate storage conditions (Fang & Bhandari, 2010) due to their volatility and sensitivity to oxygen, light or heat (Shao et al., 2018). Moreover, its incorporation into aqueous systems, such as most foods, is limited by its low water solubility and impact on flavor (Choi, Soottitantawat, Nuchucha, Min & Ruktanonchai, 2009). Most of these problems can be overcome by using encapsulation techniques, allowing for the easier handling of the active compound, a better protection during storage and transportation and a better control in the release (Bae & Lee, 2008). Spray drying is

one of the most widely used technique in encapsulation, being economical and the most feasible from the industrial point of view. Nevertheless, the composition of the aqueous phase must be optimized in order to ensure the formation of a good shell material, entrapping the active compound in the core, after the drying process; this allows for its controlled release when the powder is incorporated into a determined matrix. Spray drying has been extensively used for the encapsulation of different bioactive ingredients, including vitamins, polyunsaturated oils, phenolic compounds, enzymes, probiotics or some other compounds with an undesirable flavor, for masking purposes (Augustin & Hemar, 2009). The effectiveness of the encapsulation process is greatly affected by the properties/stability of the initial dispersion/emulsion of the active compound and, consequently, by the wall materials used in their formulation (Bae et al., 2008; Ré, 1998; Shao et al., 2018). In addition to the encapsulating efficiency, the antimicrobial or antioxidant properties of the encapsulated compound in the final dried capsules is affected by its total load in the powder (active/support compounds ratio) and its release kinetics into a determined target medium into which it could be incorporated. All these factors define the effective concentration on the target point, which must be studied to ensure the required functionality.

The components of encapsulation matrices for food application purposes are limited to edible, preferably inexpensive, materials, biopolymers being the ideal candidates meeting these requirements. Proteins, polysaccharides and polar lipids such as lecithin have been proposed as promising vehicles for the protection and/or delivery of bioactive ingredients. Proteins, such as whey protein are usually incorporated to promote emulsion formation and interfacial stabilization in the capsule-forming dispersions. The chemical structure of lecithin allows for the formation of liposomes which can entrap different kinds (more or less polar) of active compounds (Liolios, Gortzi, Lalas, Tsaknis & Chinou, 2009). At neutral pH, phosphate and carbonyl groups from phosphatidylcholine and phosphatidylethanolamine components in lecithin contribute to the negative charge of the particles in the emulsion, thus contributing to

emulsion stability by charge (Dickinson, 1993). Polysaccharides can act as stabilizers by increasing the viscosity of the continuous phase or by means of the development of electrostatic interactions at the oil-water interface. In this sense, positively charged chitosan molecules in acid media could enhance the stability of the dispersion by means of a viscous electro-steric effect at the interface, thus promoting dispersion stability (Rodríguez, Albertengo & Agullo, 2002). Maltodextrins can improve the properties of the capsules during the drying stage due to the formation of a larger crust around the drops, thus providing good protection against oxidation (Sheu & Rosenberg, 1998). Whey protein isolate (WP) or LE together with MD could form good wall systems able to stabilise in oil droplets in the oil-water emulsions, favouring the formation microcapsules during the emulsion spray drying (Karadag, Özçelik, Sramek, Gibis, Kohlus, Weiss, 2013).

On the other hand, the use of lipophilic carriers (such as oleic acid) to favor the dispersion of poorly water-soluble lipid active agents or to favor its retention after processing have reported by several authors (Woo, Mirsan, Lee & Tan, 2014; Perdones, Vargas, Atarés & Chiralt, 2014).

The aim of this study was to encapsulate eugenol by spray drying using WP or LE as wall-materials and to characterize the different formulations before (emulsion properties) and after drying, in terms of the encapsulation efficiency, thermal stability, release kinetics and antioxidant and antimicrobial activities. The effect of the incorporation of both oleic acid (OA), as eugenol carrier, and chitosan (CH), as a potential stabilizer, on the properties of the encapsulating systems was analysed.

2. Material and Methods

2.1. Raw materials

Soy lecithin (LE) Lipoid S45 from Lipoid GmbH (batch 574510, Ludwigshafen, Germany); whey protein isolate (WP) Prodiet 90S (95% whey and 1.5% fat) from Ingredia (batch 131848, France); maltodextrin (MD) Kyrosan E18 1910 QS (DE19.2, batch 02157372, Emsland Group, Germany); purified oleic acid (OA) (77% C18:1; 11% C18:2; 4% C16:0; 1% C16:1; 3% C18:0) from VWR Chemicals (Germany) and high molecular weight chitosan (CH) from Sigma-Aldrich (Madrid, Spain) were used to encapsulate pure eugenol (E), also from Sigma-Aldrich (batch STBD6235V, Madrid, Spain).

Sodium hydroxide (Merck, Darmstadt, Germany), boron trifluoride in methanol and sodium chloride (Sigma–Aldrich, Steinheim, Germany), sodium sulphate (purity 99%, VWR International, West Chester, PA, USA), C19:0 methyl ester and a GLC-63 mixture of fatty acid methyl esters (Nu-Check Prep, Elysian, MN, USA) as reagents and heptane and 2-propanol (Rathburn Chemicals Ltd., Walkerburn, Scotland) as HPLC grade solvents were used for the chromatographic fatty acid analysis. Glacial acetic acid, absolute ethanol and methanol and diphosphorus pentoxide (P_2O_5) were purchased from Panreac AppliChem (Barcelona, Spain) and 2,2-Diphenyl-1-pikryl-hydrazyl and Folin-Ciocalteu reagent were obtained from Sigma-Aldrich (Madrid, Spain), in order to determine the other assays.

2.2. Emulsion preparation

Whey Protein Isolate (WP) or Lecithin (LE) were mixed with Maltodextrin in a WP/LE:MD ratio of 1:42 (w/w) to obtain aqueous dispersions (43g solids/100g). After leaving these aqueous solutions overnight under stirring, 3% eugenol (w/w) was added, obtaining the formulations E-WP and E-LE (Table S1). 7 wt. % of oleic acid was added in formulations EOA-WP, EOA-LE, EOA-WPCH and EOA-LECH (Table S1). All of the dispersions were homogenized with a Rotor Stator (Ultra-Turrax T 25 Basic, IKA Werke GmbH & Co. KG, Germany) at 11,000 rpm for 6 minutes and

microfluidized (three cycles) with the high-pressure homogenizer (Microfluidics M-110Y, Newton, Massachusetts, USA) at 15,000 psi pressure (103,42 MPa). Formulations with CH (EOA-WPCH and EOA-LECH) were obtained by previously dispersing 1% (w/w) chitosan (CH) in 1% (v/v) acetic acid solution for 14 h, under stirring at 150 rpm. The chitosan solution was added to formulations in a CH solution:emulsion ratio of 1.5:10.

2.3. Spray-drying

All of the emulsions were spray dried by a Mobile Minor TM spray-dryer (GEA Niro, GEA Process Engineering A/S, Søborg, Denmark) with a two-fluid atomizer (co-current two-fluid nozzle system). Samples were introduced into the drying chamber at an initial flow rate of 20 mL/min and an inlet air temperature adjusted to 180 °C. The outlet temperature was kept at 80 ± 2 °C by controlling the feed rate using a peristaltic pump (Watson Marlow 520s IP31, head type 314, Watson-Marlow Bredel Pumps, Cornwall, UK). During spray-drying the fan speed was set to 2,800 rpm and the atomization air flow pressure, 1.9 bar. After spray-drying, powders were vacuum-packaged in polypropylene bags and stored under refrigeration and dark conditions until further analysis were carried out.

2.4. Characterization of the emulsions

2.4.1. Z-potential

The Z-Potential of the emulsions was measured in triplicate by using a dynamic light scattering instrument capable of measuring electrophoretic mobility (Zetasizer nano ZS, Malvern Instruments, Worcestershire, UK). The E-LE formulation was measured without dilution. The rest

of the emulsions were diluted to reach a final concentration of 1% (w/w) to prevent multiple scattering effects.

2.4.2. Particle size

The technique of laser diffraction was used to determine the size of particles in emulsions (Mastersizer 3000, Malvern Instruments). The Mie theory was applied by considering refractive and absorption indexes of 1.48 and 0.01, respectively. Samples were diluted in de-ionised water at 2500 rpm until an obscuration rate of 10% was obtained. D_{32} (surface weighted mean diameter) and D_{43} (volume weighted mean diameter) parameters were obtained. Light microscopy images of the emulsions were taken using a light microscope (Olympus, GWB MTV-3, Japan) with a digital camera.

2.4.3. Rheological behaviour

The rheological behaviour of emulsions by six-fold at 20°C were characterized. The flow curves (apparent viscosity as a function of shear rate) of emulsions were determined by ThermoHaake Rheostress 600 rheometer (Thermo Electron GmbH, Dreieich, Germany) equipped with rotating cone of 35 mm in diameter and cone angle of 1°, over a shear rate range of 0.03–100–0.03 s^{-1}. Ostwald model was fitted to the flow curves.

2.5. Characterization of the spray-dried powders

2.5.1. Particle size and microstructure (SEM)

The particle size of the spray-dried powder formulations was measured by the laser diffraction technique (Mastersizer 3000, Malvern Instruments, UK), equipped with a dry dispersion unit. A refractive index of 1.48 and an absorption of 0.01 was also considered. Samples were fed into the system at a feed rate of 60% and a pressure of 2.2 bar until an obscuration rate was obtained within the range of 0.5-6%. The parameters, $D_{3.2}$ and $D_{4,3,}$ were obtained.

The microstructure of the microcapsules was evaluated by means of scanning electron microscopy (SEM) (JEOL, JSM-5410, Japan). The powders were previously conditioned in a desiccator with diphosphorus pentoxide (P_2O_5) and they were mounted on copper stubs with double-sided adhesive carbon tape and gold coated. The images were captured by using an acceleration voltage of 15kV at 1,500 magnification.

2.5.2. Thermogravimetric analysis

To evaluate the thermal stability of the samples, both powders and pure compounds, a thermogravimetric analysis (TGA) (Star^{e}System, Mettler Toledo Inc., Switzerland) was performed. The TGA was carried out from 50°C to 600°C at a heating rate of 10°C/min under a nitrogen atmosphere (20 mL/min). Sample weight versus temperature curves were recorded using the STAR^e software of (Version 9.01, Mettler Toledo) in triplicate. The samples were previously conditioned in a desiccator with P_2O_5 until constant weight.

2.5.3. Concentration of eugenol in the powders and encapsulation efficiency

Spectrophotometric analysis was used to analyze the concentration of encapsulated eugenol in the dried formulations, previously submitted to methanol extraction. 0.1 g of sample were weighed using an analytical balance (ME36S, Sartorius,Germany; ±0.00001 g) and extracted in 100 mL of methanol under constant stirring for 24h (previously determined maximum time of

extraction). Then, the absorbance of the filtered samples was measured in triplicate, by using a spectrophotometer (ThermoScientific spectrophotometer Evolution 201 UV–vis) at 282 nm (maximum eugenol absorption in methanol). The extract of the corresponding control without eugenol was used as a blank in each case. The calibration curve (y=0.018·x; R^2=0.998) was obtained from the absorbance measurements of standard solutions of eugenol and was used to determine the concentration of eugenol in the samples.

The encapsulation efficiency (%EE) was calculated by using Equation 1, where C_E was the amount of eugenol determined by methanol extraction and $C_{theoretical\ E}$ was the theoretical eugenol content.

$$\%EE = \frac{C_E}{C_{theoretical\ E}} \cdot 100 \qquad \text{Equation 1}$$

2.5.4. Extraction and quantification of the lipid content in the whole particles and on their surface.

The surface and total lipids were extracted using the methodology described by Damerau et al. (2014). First, samples (0.3 g) were washed with 5 mL of heptane by means of a mild shaking in an orbital shaker for 15 min and then centrifuged at 2,000 rpm for 2 min. For the extraction of total lipids, 0.3 g of sample were re-suspended in 3 mL of water at 40°C and vortexed. The lipids were extracted by shaking in an orbital shaker for 15 min using 10 mL of a heptane/2-propanal mixture (3:1, v/v). After shaking, the mixture was centrifuged at 3000 rpm for 2 min and the organic phase was collected.

The fatty acid composition of the lipid extracts (both surface and total lipids) was analysed by using the method described by Damerau et al. (2014). This method is based on the saponification of the sample, followed by the methylation of the liberated fatty acids in the presence of boron trifluoride. All samples were analyzed by using a Hewlett Packard 5890 Series II GC (Karls-ruhe,

231 Germany) equipped with an automated on-column injection system and a flame ionization
232 detector (FID). The conditions were as follows: column, 60 m × 0.32 mm i.d., 0.10 µm, Rtx-5 w/
233 Integra Guard (crossbond 5% diphenyl-95% dimethyl polysiloxane) capillary column (from
234 Restek); carrier gas, helium (>99.996%) at a constant flow of 1.4 mL/min; temperature program,
235 70 °C (1 min), 60 °C/min to 245 °C (1 min), 3 °C/min to 275 °C (32 min); detector temperature,
236 300 °C. The fatty acid methyl esters were identified through the retention times by comparison
237 to a standard GLC-63 mixture of fatty acid methyl esters and quantified through the peaks' areas
238 by means of the internal standard method, (C19:0 methyl ester as the internal standard). The
239 content of each fatty acid was determined, and referred per g of solid powder, and the total
240 lipid content was estimated from the total sum of all fatty acids.
241
242 **2.6. Release Kinetics of eugenol from powders into food simulants**
243
244 Four different food simulants were used for the release studies: 3% (w/v) acetic acid (B); 10%
245 (v/v) (A), 20% (v/v) (C) and 50% (v/v) (D1) ethanoic solutions. 0.1 g of each sample was placed
246 into flasks containing 100 mL of each simulant. Release studies were carried out throughout 90
247 minutes at 25°C, using a spectrophotometric method, at 282 nm of wavelength (where the
248 eugenol absorbance is maximum), to determine the released E at different times (1, 3, 5, 7, 10,
249 15, 20, 30 and 90 minutes). The assay was performed in triplicate. The results were expressed
250 as the amount of eugenol per gram of dried powder (mg /g powder). The amount of eugenol
251 released at each time (M_t) was fitted to Peleg's model (Peleg, 1988), described by Equation 2,
252 and parameters k_1 (inverse of the initial release rate) and k_2 (inverse of the asymptotic value)
253 were obtained. The delivered amount at equilibrium (M_∞) was deduced from k_2 (Equation 3). M_0
254 =0, since no E was initially present in the simulants.
255

256 $$M_t = M_0 + \frac{t}{k_1 + k_2 t}$$ Equation 2

257

258 $$M_\infty = \frac{1}{k_2}$$ Equation 3

259

260 **2.7. Antioxidant activity**

261

262 The antioxidant capacity of the powders was determined by using a 2,2-Diphenyl-1-pikryl-
263 hydrazyl (DPPH) reduction method, following the methodology described by Brand-Williams,
264 Cuvelier & Berset (1995). In this method, the stable free radical, $DPPH^{\cdot}$, which absorbs at 515
265 nm, disappears after accepting an electron or hydrogen radical from the antioxidant
266 compounds. For this purpose, 0.1 g of powder was dispersed in 100 mL of methanol under
267 stirring for 30 minutes. Different volumes of the dispersions were reacted with a 0.06 mM
268 methanol solution of $DPPH^{\cdot}$. The absorbance measurements were taken in triplicate at 25°C
269 after 2 hours, when the reaction (absorbance at 515 nm) reached a plateau by using a
270 spectrophotometer (Thermo-Scientific spectrophotometer Evolution 201 UV-visible). The $DPPH^{\cdot}$
271 concentration (mM) in the reaction medium was determined from the calibration curve
272 (Equation 4) determined by linear regression (R^2 = 0.997). The reduction percentage in $DPPH^{\cdot}$
273 concentration ($\%DPPH^{\cdot}_{rem}$) was calculated using Equation 5.

274

275 $$Abs_{515nm} = 11.793 \cdot [DPPH^{\bullet}]$$ Equation 4

276

277 $$\%[DPPH]_{rem} = \frac{[DPPH^{\bullet}]_{t=2h}}{[DPPH^{\bullet}]_{t=0}} \cdot 100$$ Equation 5

278

where, $[DPPH^{\cdot}]_{t=2h}$ is the concentration of $DPPH^{\cdot}$ at the equilibrium time and $[DPPH^{\cdot}]_{t=0}$ is the initial concentration. From these values, the parameter EC_{50} (the antioxidant concentration required to reduce the initial [DPPH] concentration to 50%: efficient concentration) was determined through the relationship between the % $[DPPH^{\cdot}]_{rem}$ and the mass ratio of powder to $DPPH^{\cdot}$ (mg powder/mg DPPH). Thus, a low value of EC_{50} is related to a higher antioxidant activity of the analysed sample. The antioxidant activity of the pure eugenol was also determined, using the same method.

2.8. Antimicrobial activity

The antimicrobial effectiveness of powders was evaluated by using an *in vitro* method adapted from Cano, Cháfer, Chiralt & González-Martínez (2015). Two bacteria, *Listeria innocua* as Gram+ and *Escherichia coli* as Gram-, were used. The bacteria were regenerated by transferring a loopful into 10 mL of TSB and incubating at 37°C overnight. A 10 µL aliquot from the overnight culture was again transferred to 10 mL of tryptic soy broth (TSB) and grown at 37°C to the end of the exponential growth phase. These cultures were diluted to approximately 5.0–6.0 log CFU/mL. Different amounts of each powder were added to test tubes containing 9 mL of TSB and 1 mL of the inoculum; the final E concentration (from the powder) ranged from 0.5 to 1.75 g Eugenol/L. The mixtures were vortexed and kept under stirring for 30 min at the optimum growth temperature. A bacterial suspension sample of 1 mL was serially diluted in water peptone and 1 mL of the dilutions were inoculated into Petri dishes in duplicate by using Violet Red Bilis agar (Sharlab S.A., Barcelona, Spain) in the case of *E. coli* cultures, and Palcam Agar Base (Sharlab S.A., Barcelona, Spain) supplemented with Palcam Selective Supplement (Sharlab S.A., Barcelona, Spain) in the case of *L. innocua*. Plate samples were incubated for 24 or 48 h at 37 °C for *Listeria* or *E. coli*, respectively, and then counted as CFU/mL.

2.9. Statistical analysis

Statgraphics Centurion XVI software (Manugistics Corp., Rockville, Md.) for Windows 5.1 (Manugistic Corp. Rockville, MD, USA) was used to carry out a statistical analysis of data through an analysis of variance (ANOVA). Fisher´s least significance difference (LSD) was used at the 95% confidence level.

3. Results and discussion

3.1. Emulsion characterization

The particle size distribution of the different formulations can be observed in Figure 1. All dispersions exhibited multimodal distributions with droplet diameters ranging from 0.1 to 100 µm, except the EOA-WP formulation, which exhibited monomodal behaviour. The E-WP based emulsion had particle size distributions between 0.5 and 100 µm, with the main peak at 10 µm. Similar particles sizes have been found by other authors using whey protein-oil-water emulsions homogenized at similar homogenization pressures (100 MPa) (Hebishy, Zamora, Buffa, Blasco-Moreno & Trujillo, 2017). However, the E-LE based emulsion showed the formation of smaller particles (main peak around 0.1 µm), which indicates the formation of lecithin nanoliposomes, although some bigger particles appeared at around 100 µm, which may be due to the formation of either some lamellar forms or some clusters of maltodextrins as a result of their high concentration in the emulsion. In fact, Gibis, Thellmann, Thongkaew & Weis (2014) obtained monomodal distributions (0.1 µm peak) using lecithin and different plant extracts submitted to higher homogenization pressures (155 MPa). The incorporation of oleic acid notably reduced ($p<0.05$) the particle sizes and promoted narrower particle size distributions in systems with WP,

331 although the curve shifted to higher size values in the LE liposome systems, probably due to the
332 OA interactions with the lipid associations of lecithin, which modify the aggregation number of
333 the lipid association structure. The amphiphilic nature of OA favours the emulsification process
334 and the reduction in the droplet particle size, as previously reported by other authors (Vargas,
335 Albors, Chiralt & González-Martínez, 2009), but the OA interactions with other polar lipids, such
336 as lecithin compounds, affect the final lipid rearrangement both on the lipid-water interface or
337 in the lipid association of micellar structures. OA interactions with WP can also imply differences
338 in the amphiphilic layer adsorbed on the lipid (E) droplets, even provoking the displacement of
339 protein from the interface due to the lower surface tension of the surfactant.
340 The incorporation of CH to WP or LE systems provoked particle flocculation, especially in the WP
341 systems, as revealed by the shift of the particle sizes towards multimodal distributions with
342 bigger particles (peaks near 100 μm, in both WP and LE systems). This effect could be due to the
343 emulsion depletion associated with the exclusion effect (McClements, 2005). However, the
344 positive charge of the polymer could also provoke an entanglement effect on the negatively
345 charged droplets revealed by their zeta potential (Table S2). In lecithin-based formulations,
346 attractive interactions between the positively-charged chitosan and the negatively-charged
347 groups of phospholipids (pK_a values of anionic phosphatidic groups are typically around 1.5;
348 Ogawa, Decker & McClements et al., 2004), at an emulsion pH of nearly 4 (Table S2), were
349 expected, leading to the formation of larger particles. In fact, the zeta potential (Table S2) of
350 CH-free EOA-LE system was -45.7 mV at the emulsion natural pH (Table S2), as reported by Gibis,
351 Vogt & Weiss (2012) at pH 3.8. This charge was inverted when CH was incorporated, leading to
352 a zeta potential of +61.5 mV.

353 In WP systems, electrostatic interactions between whey protein and chitosan were not
354 expected, since the isoelectric point (IP) of whey protein is around 4-5 (Giese, 1994) and,
355 although the zeta potential of the WP emulsions at their natural pH (nearly 6) was negative, the
356 incorporation of a CH solution decreased the pH to about 4 and the zeta potential became

positive. The CH-free WP systems also exhibited positive zeta potential at this pH (4) as shown in Table S2, according to the IP of the protein. Moreover, at pH values close to the WP isoelectric point, the solubility of protein is limited which can lead to emulsion flocculation by solvent effect (McClements, 2005). Therefore, the use of chitosan promoted a greater polydispersity in the particle size distributions and the formation of bigger particles, associated with different aggregation phenomena, especially in WP-based dispersions. Light microscopy images in Figure 1 show the different droplet sizes in the emulsions, coherent with the distributions commented on above. The flocculated particles and large lipid droplets can be clearly observed, reflecting the occurrence of coalescence, associated with the emulsion destabilisation provoked by CH addition in both WP and LE systems.

All emulsions exhibited pseudoplastic rheological behaviour. Table S2 also shows the values of the rheological parameters (flow index: n and consistency index: K) and the apparent viscosity of the different emulsions at 50 s^{-1}. All CH-free dispersions almost presented Newtonian behaviour (n close to 1), whereas the incorporation of CH promoted a more pseudoplastic pattern. The incorporation of OA did not produce significant changes in the rheological behaviour or viscosity of the dispersions (Table S2) ($p>0.05$). An increase in the emulsion consistency could be expected in line with the higher volume fraction of the dispersed phase, but the reduction in the particle size promoted by OA or its efficient incorporation into WP micelles or LE-liposomes could mitigate this effect. The dispersions turned more shear-thinning and viscous with the addition of CH, in agreement with the formation of large aggregates whose coarse structure would be more sensitive (e.g. disaggregation or deformation of large droplets) to the shear rate.

3.2. Powder encapsulate characterization

382 The morphology of the particles obtained by spray-drying depends on several factors, such as
383 the drying kinetics and the liquid phase composition. At the beginning of the drying process, the
384 surface of the atomized droplets begins to dry, forming a crust, then bubble nucleation occurs,
385 and bubbles grow, enlarge and burst out through the surface until most of the internal moisture
386 has evaporated (Rosenberg, Kopelman & Talmon, 1990). Since the drying conditions were
387 constant for every formulation, the different morphology observed for dried particles (Figure 2)
388 would only be affected by their composition. Factors, such as the film-forming properties of the
389 drying carrier and the interactions of the wall material with the active substance (eugenol), could
390 affect the morphology of the solid particles. Eugenol encapsulated in LE or WP (no OA or CH
391 present) produced particles with irregular surfaces over a wide range of sizes, which is typical of
392 low-loaded capsules. Surface irregularities suggest the swelling of the rubbery particle surface
393 in the initial drying stages due to the internal pressure of the water vapour, which collapses
394 when the internal vapour pressure decreases as a result of the lower volume of the internal lipid.
395 Ré (1998) associated these particle shapes with a slow surface film formation during drying in
396 the atomized droplet. Similar morphological characteristics were found by Carneiro, Tonon,
397 Grosso & Hubinger (2013). In contrast, when the formulations contained OA as eugenol carrier,
398 the particles became more spherical in shape with fewer surface irregularities, due to the
399 presence of OA inside the particles (0.134 mass fraction in the powder, against 0.06 of E), which
400 limits the further shrinkage of the non-lipid shell. As expected, bigger particles and large
401 agglomerates were observed in systems containing chitosan. No notable differences in the
402 particle appearance were observed when using LE or WP as wall materials, although in the WP
403 systems a slightly higher degree of particle aggregation could be appreciated in the powder, thus
404 indicating greater attractive forces between dry particles.

405 The particle size distributions of the different powder formulations can be observed in Figure 2.
406 As can be observed, all chitosan-free formulations exhibited very similar, “almost” monomodal,
407 distributions with a mean particle diameter of around 15 μm, regardless of the wall material

(WP or LE). A very small shoulder, corresponding to the finest particles (around 0.5 µm), was also observed in both systems. This is particularly interesting in the case of powders, as the population of smaller particles can penetrate the spaces between the larger ones, thus giving rise to powders with higher apparent density during the powder compaction (Carneiro et al., 2013).

The addition of chitosan shifted the particle size distributions towards larger sizes, exhibiting a multimodal pattern, as was also observed in SEM micrographs. Two main populations, showing peak values of 20 and 170 µm for EOA-WPCH and of 30 and 150 µm for EOA-LECH formulations, were observed. The high viscosity and larger particles of these emulsions could limit the jet disruption in smaller droplets during the spray drying process. Several authors (Augustin & Hemar, 2009; Bae & Lee, 2008; Carneiro et al., 2013; McClements, 2005) reported that the atomized droplet size depends directly on the emulsion viscosity at a constant atomization speed. The greater the emulsion viscosity, the larger the droplets formed during atomization, and consequently, the larger the particles in the obtained powder.

Table S3 shows the moisture content and onset and peak temperatures from the TGA analysis of powder encapsulates. The different formulations exhibited moisture contents ranging between 1.7 to 3 g water/100 g dry powder.

The TGA and DTGA curves of the different samples are shown in Figure 3. Two different weight loss steps were observed below 250ºC. The first one, below about 100 ºC, must be attributed to the evaporation of the powder water content (He, Hong, Gu, Liu, Cheng & Li, 2016), while the small peaks (shoulders) in DGTA curves, at about 200-250 ºC, reflect the evaporation of eugenol (254ºC boiling point) from the powder. The main thermodegradation step corresponds to the thermal degradation of the major compounds in the matrix (maltodextrins: 0.8-0.9 mass fraction in the powder), affected by their interactions with the other minor, non-volatile components (WP, LE, OA or CH). In Figure 3, the thermal degradation behaviour of pure components was also

shown to facilitate the analysis of the component interaction effect on the thermal degradation of the different encapsulates. In the case of maltodextrins, the peak temperature of the maximum degradation rate is at 286 °C, whereas in the powder encapsulates, these temperatures were about 283 and 260 °C, for matrices containing WP and LE, respectively.. No practical effect of WP was observed on the thermal behaviour of maltodextrin matrices, whereas LE notably decreased the thermal stability of the powder. The WP powders degraded at a higher temperature than the LE, due to the proteins contribution to the increase in the mean molecular weight of the maltodextrin matrix and the subsequent enhancement of the cohesive forces through the entanglement effect of the protein chains. In contrast, the LE lipids reduce the thermal stability of the matrix, probably due to the plasticizing effect of the lipids, which reduce the attractive forces between the carbohydrate chains, weakening the network cohesion. OA or CH slightly affected the thermal degradation temperature of the WP powders, but the only significance is to be found in the small decrease provoked by OA, which could also be associated with its plasticizing effect in the matrix (Fabra, Talens & Chiralt, 2010). In the LE based systems, the CH or OA incorporation did not have a significant effect on the thermal stability of the material.

As regards the loss of eugenol from the encapsulant matrix, associated to its thermal release, the behaviour of the powders was remarkably different. A clear peak (maximum evaporation rate) was observed at about 200 ^{o}C for samples containing CH, whereas the compound thermal release appeared at about 240 ^{o}C in WP systems with and without OA (respective shoulders in DGTA curves). In LE powders, the E thermal release overlapped with the degradation temperature range of the matrix and no specific E weight loss event was observed in the DGTA. In contrast, for free eugenol submitted to the same thermal test, the maximum evaporation rate occurred at 175 ^{o}C. These results reflect the different protective effect of the encapsulates when it is a matter of limiting the loss of E from the powder, the LE systems without CH being the most effective at retaining E in the matrix. The incorporation of CH into the encapsulates implied less

459 protection against the evaporation of E, which suggests a poor inclusion of the compound in the
460 particle core, but probably a greater presence on the particle surface. Additionally, the thermal
461 stability of the encapsulated materials allows for their incorporation into different products
462 submitted to thermal processing, involving temperatures lower than 175 ^{o}C or 200 ^{o}C, for
463 powders with or without CH, preventing the potential thermal release of eugenol, as previously
464 observed by other authors (He et al., 2016).
465 In order to know the encapsulation efficiency (EE) of eugenol, its total content in each powder
466 sample was determined and compared with the theoretical incorporated amount (Table S1).
467 Table 1 shows the different EE values for each sample. EE was very high (around 94-99%) when
468 using only WP or LE as wall materials. These values were higher than those found by other
469 authors encapsulating eugenol with solid lipid nanoparticles (SLN) (Cortes-Rojas et al., 2014),
470 and similar to those found by Seo, Min & Choi (2010) using β-cyclodextrin. The incorporation of
471 OA into the emulsions slightly decreased the EE values, only being significant in the EOA-WP
472 samples. On the other hand, the use of chitosan remarkably reduced ($p<0.05$) the EE values to
473 22 and 46% for WP and LE systems, respectively. The presence of free OA containing eugenol on
474 the surface of the dried particles (Table 1) could explain the lower EE values, especially in the
475 samples containing CH. To verify this hypothesis, the total and surface lipid contents were
476 analysed, as described in section 2.5, through the analyses of fatty acids present in the whole
477 particles (total lipid content: TLC) and on their surface (surface lipid content: SLC).

478 Table S4 shows the TLC and SLC, and the specific content of the different fatty acids found in
479 each spray-dried particle. Particles from LE systems contained a higher fat content and different
480 fatty acid profiles (both in TLC and SLC) than those from WP systems, in line with the lecithin
481 composition. As expected, the TLC values were always higher than the SLC, indicating the
482 predominant location of lipids in the internal core of the particles, with a partial retention at
483 surface level. WP based samples without OA had a very low lipid content, coming from the raw
484 WP powder, and about 40 % were on the particle surface. In the rest of the samples, the TLC

quantified through the total fatty acids was, as expected, lower than the theoretical lipid load in the powders (OA and/or LE), although in samples containing OA the values were very close, since this component was present at a higher ratio than LE (Table S1). However, the percentage of the SLC with respect to TLC greatly differed from powder to powder. Whereas only 4.5 and 3.5 % was present on the particle surfaces of OA loaded WP and LE systems, respectively, powders with CH contained 65 and 54 % of the total lipids on the particle surface, in WP and LE systems, respectively. These results indicate that most of the lipids carrying eugenol were entrapped in the internal core of the dried particles, except when CH was incorporated into the emulsions, where a very high ratio of lipids was present on the particle surface. This could be attributed to the greater instability of the flocculated emulsions, which promotes the oil droplet coalescence during the spray drying process, reaching larger sizes than the atomized droplets. In this context, the lipid phase was not efficiently entrapped in the core of the dried particles, but extended/adsorbed on their surface, also carrying eugenol to the particle surface, from which it could easily evaporate. This behavior explains the much lower EE values for eugenol in powders containing CH.

Figure S1 shows the profile of major fatty acids (individual content with respect to the total content) in the whole particles and on their surface, compared with the typical profile of the raw OA component. Powders with OA (EOA-WP, EOA-LE, EOA-WPCH and EOA-LECH) exhibited a very similar profile at internal and surface levels. This was also very close to that of the raw OA, due to its higher mass fraction in the powder. This suggests that there was no notable amount of the LE lipids present on the particle surface and most of the formed liposomes were entrapped in the particle core, carrying most of the incorporated eugenol. In samples without OA, significant differences were observed in the fatty acid profiles of the particle surfaces and whole particles, according to the specific surface adsorption capacity of the different lipids of raw LE or WP products. This was particularly notable in OA-free LE samples, where LE lipid fractions containing more OA were predominantly adsorbed on the particle surface.

511 It can be assumed that the eugenol carried by the surface lipids quickly evaporates, mainly
512 during the spray drying process, due to the lack of a true encapsulation, decreasing the total
513 content in the powder or the EE. Taking into account the SLC values, and considering that most
514 of the surface lipids come from the incorporated OA component, the loss of eugenol during the
515 drying process was estimated from the E:OA ratio in the emulsions. In this sense, around 4 and
516 3% of the incorporated eugenol would be present on the particle surface in EOA-WP and EOA-
517 LE samples, respectively, whereas 60 and 50% of the incorporated E would be on the particle
518 surface in EOA-WPCH and EOA-LECH formulations. The sum of the encapsulated and surface
519 eugenol was nearly 100 % of the incorporated E in every case, which verifies the hypothesis that
520 only when lipids carrying E exhibited small droplet size in the initial emulsions, was the EE high
521 and a great amount of the compound could be retained in the powder. Therefore, all the factors
522 contributing to a reduction in droplet size and emulsion stability will favour the EE in the spray
523 drying processes. The less efficient retention of E in powders containing CH during its thermal
524 release, deduced from the TGA analyses, is also coherent with the higher degree of instability of
525 the emulsions containing CH.

526

527 **3.3. Release Kinetics**

528 As concerns the release kinetics of the encapsulated E from the different formulations into food
529 simulants of differing polarity, Figure 4 shows the percentage of eugenol released (% M_t/M_0,
530 where M_t is the amount of eugenol released at each time and M_0 is the initial eugenol content)
531 as a function of time for LE powders. Very similar behaviour was observed for WP-based
532 formulations (data not shown). The experimental data (points) and curves predicted (lines) by
533 the fitted Peleg model are shown. Table S5 shows the parameters of the Peleg model, where k_1
534 is the kinetic constant of the model (min/(mg E/g powder)) related to the mass transfer rate at
535 the beginning of the process and k_2 is related to the asymptotic value of the curve or amount

released at equilibrium ($1/k_2=M_\infty$, mg eugenol/g powder). The maximum release ratio (M_∞/M_0) was estimated with respect to the total methanol extracted eugenol (M_0) in each powder. A good fit of the model was obtained in every case, as reflected by the R^2 values in Table S5.

All powders released practically their total content of E at equilibrium (M_∞) (M_∞/M_0 ranged between 84-100%) in the tested aqueous simulants, as shown in Table S5. This suggests that the release of the active agent was not notably affected by pH or polarity of the food simulant. No significant differences in the M_∞/M_0 values were found ($p>0.05$) due to the use of different simulants or wall materials. As concerns the eugenol release rate (inverse of K_1), no significant effect of the wall material (WP or LE) ($p>0.05$) was observed, but the release rate significantly decreased when incorporating OA and CH, obtaining the slowest rates in formulations containing chitosan (greatest k_1 values). This CH effect could be attributed to the lower content of encapsulated eugenol in these formulations, which implies a minor driving force for the release. In general, the different simulants were found to have no significant effect on the K_1 values of a determined sample, exhibiting a burst eugenol release throughout the first 20 min. The behaviour observed is coherent with the high water affinity/solubility of the shell material, which favours the fast disruption of the capsules with the subsequent release of the E content.

3.4. Antioxidant and antibacterial activity

All powders exhibited antioxidant and antimicrobial activities to some extent, depending on the eugenol content in each sample. The antioxidant activity was evaluated in terms of EC_{50} values. This parameter indicates the amount of sample needed to halve the DPPH radical amount. Thus, the lower the EC_{50} values, the greater the antioxidant activity. In Table 1, the EC_{50} values of the different formulations, together with the pure eugenol, are shown. Pure eugenol showed the lowest EC_{50} value, 0.22 mol eugenol/mol DPPH, which was similar to that previously reported by Brand-Williams et al. (2005). The EC_{50} values of CH-free powders (expressed in terms of moles

561 of eugenol in the powder per mol DPPH) were in the range of the pure component. These results
562 reflected the fact that the antioxidant activity of eugenol was efficiently preserved during the
563 drying process when using lecithin or whey protein as wall materials, with or without OA as
564 carrier agent. However, powders with CH exhibited higher EC_{50} values (lower antioxidant
565 activity), referred to their E content, which could be due to the partial oxidation of the
566 compound retained in the external zone of the particles (surface lipids).

567 The antimicrobial activity of the samples was evaluated against one Gram – bacterium (*E. coli*)
568 and one Gram + (*L. innocua*). Powders with CH did not exhibit antibacterial effect at any
569 concentration tested, which may be explained by their low eugenol content, which did not
570 exceed the MIC of either bacterium in any case. In Figure 5, the bacterial growth inhibition of
571 the CH-free powders as a function of the powder concentration (mg powder/mL) can be
572 observed. No significant differences were found between WP and LE systems and, therefore,
573 the mean values for a determined powder concentration are shown in Figure 5 for powders with
574 and without OA. As expected, the CH-free samples exhibited a dose-dependent antimicrobial
575 activity against both bacteria. Formulations were more effective against *E. coli* than against *L.*
576 *innocua,* in agreement with that previously reported by Gaysinsky, Davidson, Bruce & Weiss
577 (2005) for eugenol encapsulated in surfactant micelles.

578 In the case of *E. coli*, OA-free powders exhibited the most marked antibacterial effect, due to
579 their greater eugenol load (Table 1). A complete growth inhibition (bactericidal effect) was
580 obtained with 15 mg /mL, which corresponds to 1 g eugenol/L. This value agrees with the MIC
581 found by other authors (Kamatou et al., 2012; Shah, Davidson & Zhong, 2013) for *E. coli* (around
582 1-1.6 g eugenol/L). The incorporation of OA into formulations significantly decreased the
583 antibacterial action, only provoking nearly a 3 Log CFU reduction when using 30 mg powder/mL.
584 As concerns *L. innocua*, both powders (with and without OA) had a similar antibacterial effect,
585 despite the different eugenol content, causing a total inhibition at about 25 mg powder/mL

(equivalent to about 1.2 or 1.6 g eugenol/L, respectively for powder with and without OA). This could be attributed to the antimicrobial activity reported for some unsaturated fatty acids (such as oleic acid) against Gram positive bacteria (Zheng, Yoo, Lee, Cho, Kim & Kim, 2005).

Conclusions

The encapsulation efficiency (EE) of eugenol in spray-dried powders containing whey protein or lecithin as wall materials and maltodextrin as drying coadjuvant was very high (95-98 %), while the incorporation of oleic acid (OA) as eugenol carrier or chitosan (CH) to the liquid formulations did not improve EE. CH provoked emulsion destabilization, which had a very negative effect on the EE. All encapsulating powders exhibited antioxidant activity, coherent with their respective eugenol content, in line with the fast, complete release of eugenol in aqueous systems. The antibacterial effect of the powders against *E. coli* was also coherent with their eugenol content, but an additional positive effect of OA was detected in the powder antilisterial action. All encapsulating powders presented small particles and a high affinity /solubility in aqueous systems of differing polarity and pH, which allows for a relatively fast, total release of the active compound. The thermal release of eugenol was also inhibited in the powders (mainly in those which were CH-free), which would allow for their use in dry thermal processes, such as the preparation of an active master batch of thermoplastic polymers. Their incorporation as an ingredient or in separate sachets in foodstuffs would permit them to be better preserved against oxidative or microbial decay, thus extending their shelf-life.

Acknowledgements

610 The authors acknowledge the financial support provided by the Spanish Ministerio de Educación
611 y Ciencia (Projects AGL2013-42989-R and AGL2016-76699-R). Author Emma Talon thanks the
612 Universitat Politècnica València (UPV) for a FPI Grant (99/2011). The authors also thank
613 Zhonqing Jiang and Tuula Sontag-Strohm from the Department of Food and Environmental
614 Sciences (University of Helsinki, Finland) for their support and assistance in the use of the
615 rheometer and Mastersizer 3000 and are very grateful for the services rendered by the Electron
616 Microscopy Service of the UPV.

617

618

619 **References**

620 Augustin, M. A., & Hemar, Y. (2009). Nano-and micro-structured assemblies for encapsulation of food
621 ingredients. Chemical society reviews, 38(4), 902-912.

622 Bae, E. K., & Lee, S. J. (2008). Microencapsulation of avocado oil by spray drying using whey protein and
623 maltodextrin. Journal of Microencapsulation, 25(8), 549-560.

624 Brand-Williams, W., Cuvelier, M. E., & Berset, C. L. W. T. (1995). Use of a free radical method to evaluate
625 antioxidant activity. LWT-Food science and Technology, 28(1), 25-30.

626 Cano, A., Cháfer, M., Chiralt, A., & González-Martínez, C. (2015). Physical and antimicrobial properties of
627 starch-PVA blend films as affected by the incorporation of natural antimicrobial agents. Foods, 5(1), 3.

628 Carneiro, H. C., Tonon, R. V., Grosso, C. R., & Hubinger, M. D. (2013). Encapsulation efficiency and oxidative
629 stability of flaxseed oil microencapsulated by spray drying using different combinations of wall materials.
630 Journal of Food Engineering, 115(4), 443-451.

631 Chatterjee, D., & Bhattacharjee, P. (2013). Comparative evaluation of the antioxidant efficacy of
632 encapsulated and un-encapsulated eugenol-rich clove extracts in soybean oil: shelf-life and frying stability
633 of soybean oil. Journal of Food Engineering, 117(4), 545-550.

634 Chatterjee, D., & Bhattacharjee, P. (2015). Use of eugenol-lean clove extract as a flavoring agent and
635 natural antioxidant in mayonnaise: product characterization and storage study. Journal of food science
636 and technology, 52(8), 4945-4954.

637 Choi, M. J., Soottitantawat, A., Nuchuchua, O., Min, S. G., & Ruktanonchai, U. (2009). Physical and light
638 oxidative properties of eugenol encapsulated by molecular inclusion and emulsion–diffusion method.
639 Food Research International, 42(1), 148-156.

640 Cortés-Rojas, D. F., Souza, C. R., & Oliveira, W. P. (2014). Encapsulation of eugenol rich clove extract in
641 solid lipid carriers. Journal of Food Engineering, 127, 34-42.

642 Damerau, A., Moisio, T., Partanen, R., Forssell, P., Lampi, A. M., & Piironen, V. (2014). Interfacial protein
643 engineering for spray-dried emulsions–Part II: Oxidative stability. Food chemistry, 144, 57-64.

644 Dickinson, E. (1993). Towards more natural emulsifiers. Trends in Food Science & Technology, 4(10), 330-
645 334.

646 Dorman, H. J. D., & Deans, S. G. (2000). Antimicrobial agents from plants: antibacterial activity of plant
647 volatile oils. Journal of applied microbiology, 88(2), 308-316.

648 Fabra, M. J., Talens, P., & Chiralt, A. (2010). Water sorption isotherms and phase transitions of sodium
649 caseinate–lipid films as affected by lipid interactions. Food hydrocolloids, 24(4), 384-391.

650 Fang, Z., & Bhandari, B. (2010). Encapsulation of polyphenols–a review. Trends in Food Science &
651 Technology, 21(10), 510-523.

652 Gaysinsky, S., Davidson, P. M., Bruce, B. D., & Weiss, J. (2005). Stability and antimicrobial efficiency of
653 eugenol encapsulated in surfactant micelles as affected by temperature and pH. Journal of food
654 protection, 68(7), 1359-1366.

655 Gibis, M., Vogt, E., & Weiss, J. (2012). Encapsulation of polyphenolic grape seed extract in polymer-coated
656 liposomes. Food & function, 3(3), 246-254.

657 Gibis, M., Thellmann, K., Thongkaew, C., & Weiss, J. (2014). Interaction of polyphenols and multilayered
658 liposomal-encapsulated grape seed extract with native and heat-treated proteins. Food Hydrocolloids, 41,
659 119-131.

660 Giese, J. (1994). Proteins as ingredients: types, functions, applications. Food technology (USA).

661 He, H., Hong, Y., Gu, Z., Liu, G., Cheng, L., & Li, Z. (2016). Improved stability and controlled release of CLA
662 with spray-dried microcapsules of OSA-modified starch and xanthan gum. Carbohydrate polymers, 147,
663 243-250.

664 Hebishy E., Zamora, A., Buffa, M., Blasco-Moreno, A., Trujillo A. (2017). Characterization of whey protein
665 oil in water emulsions with different oil concentrations stabilized by ultra-high pressure homogenization.
666 Processes 2017, 5(1), 6; doi:10.3390/pr5010006.

667 Karadag, A., Özçelik, B., Sramek, M., Gibis, M., Kohlus, R., & Weiss, J. (2013). Presence of electrostatically
668 adsorbed polysaccharides improves spray drying of liposomes. Journal of food science, 78(2).

669 Liolios, C. C., Gortzi, O., Lalas, S., Tsaknis, J., & Chinou, I. (2009). Liposomal incorporation of carvacrol and
670 thymol isolated from the essential oil of Origanum dictamnus L. and in vitro antimicrobial activity. Food
671 chemistry, 112(1), 77-83.

672 McClements, D. J. (2005). Theoretical analysis of factors affecting the formation and stability of
673 multilayered colloidal dispersions. Langmuir, 21(21), 9777-9785.

674 Ogata, M., Hoshi, M., Urano, S., & Endo, T. (2000). Antioxidant activity of eugenol and related monomeric
675 and dimeric compounds. Chemical and Pharmaceutical Bulletin, 48(10), 1467-1469.

676 Ogawa, S., Decker, E. A., & McClements, D. J. (2004). Production and characterization of o/w emulsions
677 containing droplets stabilized by lecithin− chitosan− pectin mutilayered membranes. Journal of
678 agricultural and food chemistry, 52(11), 3595-3600.

679 Perdones, Á., Vargas, M., Atarés, L., & Chiralt, A. (2014). Physical, antioxidant and antimicrobial properties
680 of chitosan–cinnamon leaf oil films as affected by oleic acid. Food Hydrocolloids, 36, 256-264.

681 Pinto, E., Vale-Silva, L., Cavaleiro, C., & Salgueiro, L. (2009). Antifungal activity of the clove essential oil
682 from Syzygium aromaticum on Candida, Aspergillus and dermatophyte species. Journal of medical
683 microbiology, 58(11), 1454-1462.

684 Prakash, B., Kedia, A., Mishra, P. K., & Dubey, N. K. (2015). Plant essential oils as food preservatives to
685 control moulds, mycotoxin contamination and oxidative deterioration of agri-food commodities–
686 Potentials and challenges. Food Control, 47, 381-391.

687 Ré, M. (1998). Microencapsulation by spray drying. Drying technology, 16(6), 1195-1236.

688 Rodríguez, M. S., Albertengo, L. A., & Agullo, E. (2002). Emulsification capacity of chitosan. Carbohydrate
689 polymers, 48(3), 271-276.

690 Rosenberg, M., Kopelman, I. J., & Talmon, Y. (1990). Factors affecting retention in spray-drying
691 microencapsulation of volatile materials. Journal of Agricultural and Food Chemistry, 38(5), 1288-1294.

692 Seo, E. J., Min, S. G., & Choi, M. J. (2010). Release characteristics of freeze-dried eugenol encapsulated
693 with β-cyclodextrin by molecular inclusion method. Journal of microencapsulation, 27(6), 496-505.

694 Shah, B., Davidson, P. M., & Zhong, Q. (2013). Nanodispersed eugenol has improved antimicrobial activity
695 against Escherichia coli O157: H7 and Listeria monocytogenes in bovine milk. International journal of food
696 microbiology, 161(1), 53-59.

697 Shao, Y., Wu, C., Wu, T., Li, Y., Chen, S., Yuan, C., & Hu, Y. (2018). Eugenol-chitosan nanoemulsions by
698 ultrasound-mediated emulsification: Formulation, characterization and antimicrobial activity.
699 *Carbohydrate polymers*, 193, 144-152.

700 Sheu, T. Y., & Rosenberg, M. (1998). Microstructure of microcapsules consisting of whey proteins and
701 carbohydrates. Journal of Food Science, 63(3), 491-494.

702 Šimović, M., Delaš, F., Gradvol, V., Kocevski, D., & Pavlović, H. (2014). Antifungal effect of eugenol and
703 carvacrol against foodborne pathogens Aspergillus carbonarius and Penicillium roqueforti in improving
704 safety of fresh-cut watermelon. Journal of intercultural ethnopharmacology, 3(3), 91.

705 Taylor, J., Taylor, J. R. N., Dutton, M. F., & De Kock, S. (2005). Identification of kafirin film casting solvents.
706 Food chemistry, 90(3), 401-408.

707 Vargas, M., Albors, A., Chiralt, A., & González-Martínez, C. (2009). Characterization of chitosan–oleic acid
708 composite films. Food Hydrocolloids, 23(2), 536-547.

709 Woo, J. O., Misran, M., Lee, P. F., & Tan, L. P. (2014). Development of a controlled release of salicylic acid
710 loaded stearic acid-oleic acid nanoparticles in cream for topical delivery. The Scientific World Journal,
711 2014.

712 Zheng, C. J., Yoo, J. S., Lee, T. G., Cho, H. Y., Kim, Y. H., & Kim, W. G. (2005). Fatty acid synthesis is a target
713 for antibacterial activity of unsaturated fatty acids. FEBS letters, 579(23), 5157-5162.

714

715

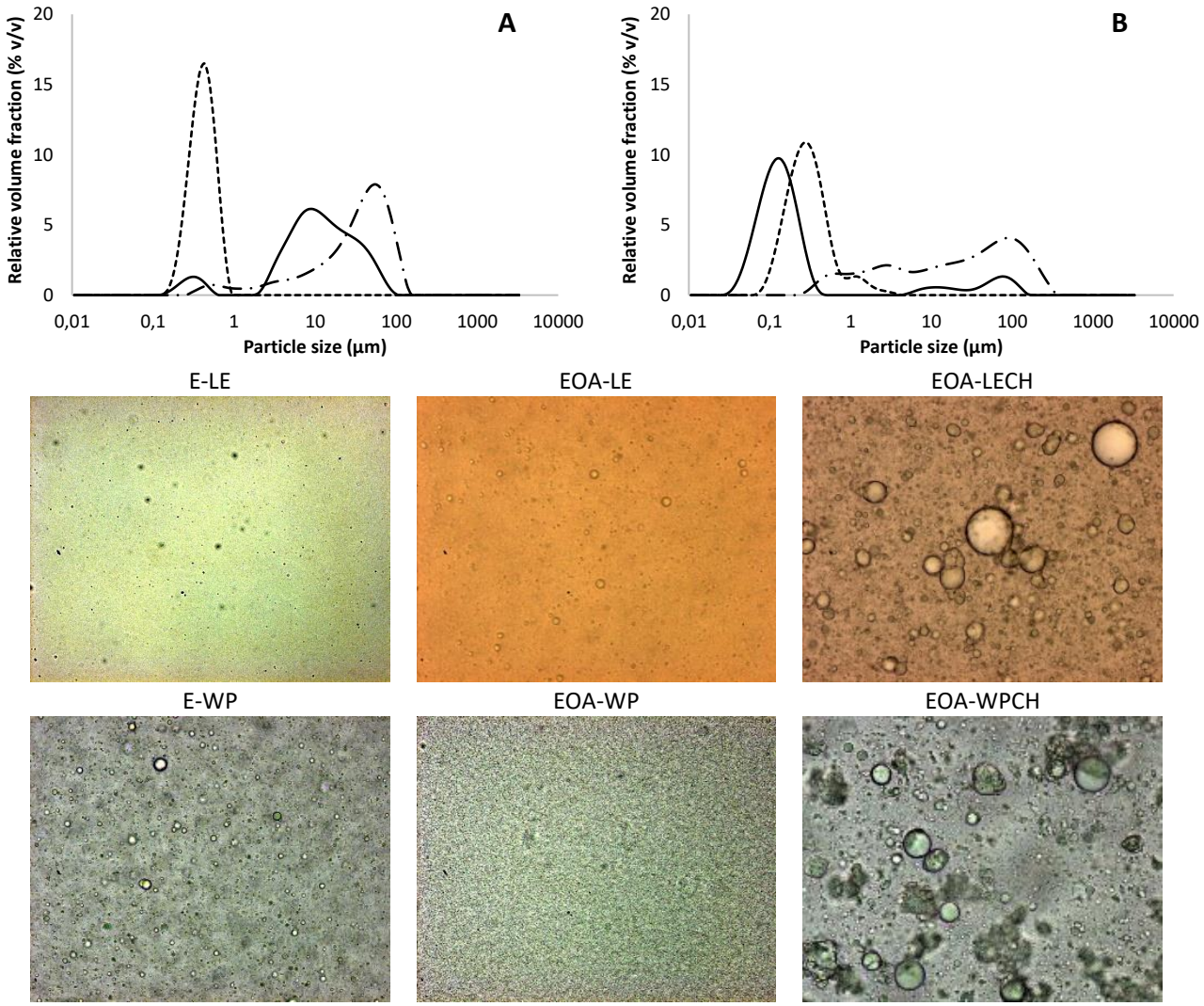

716 **Figure 1.** Typical particle size distributions of eugenol (E) emulsions using whey protein (A) or lecithin (B)

717 as wall materials, incorporating or not oleic acid (OA) and chitosan (CH) (—— E; ----EOA; — · — · EOA-CH).

718 Light microscopy images (x40) of the different emulsions are also shown.

719

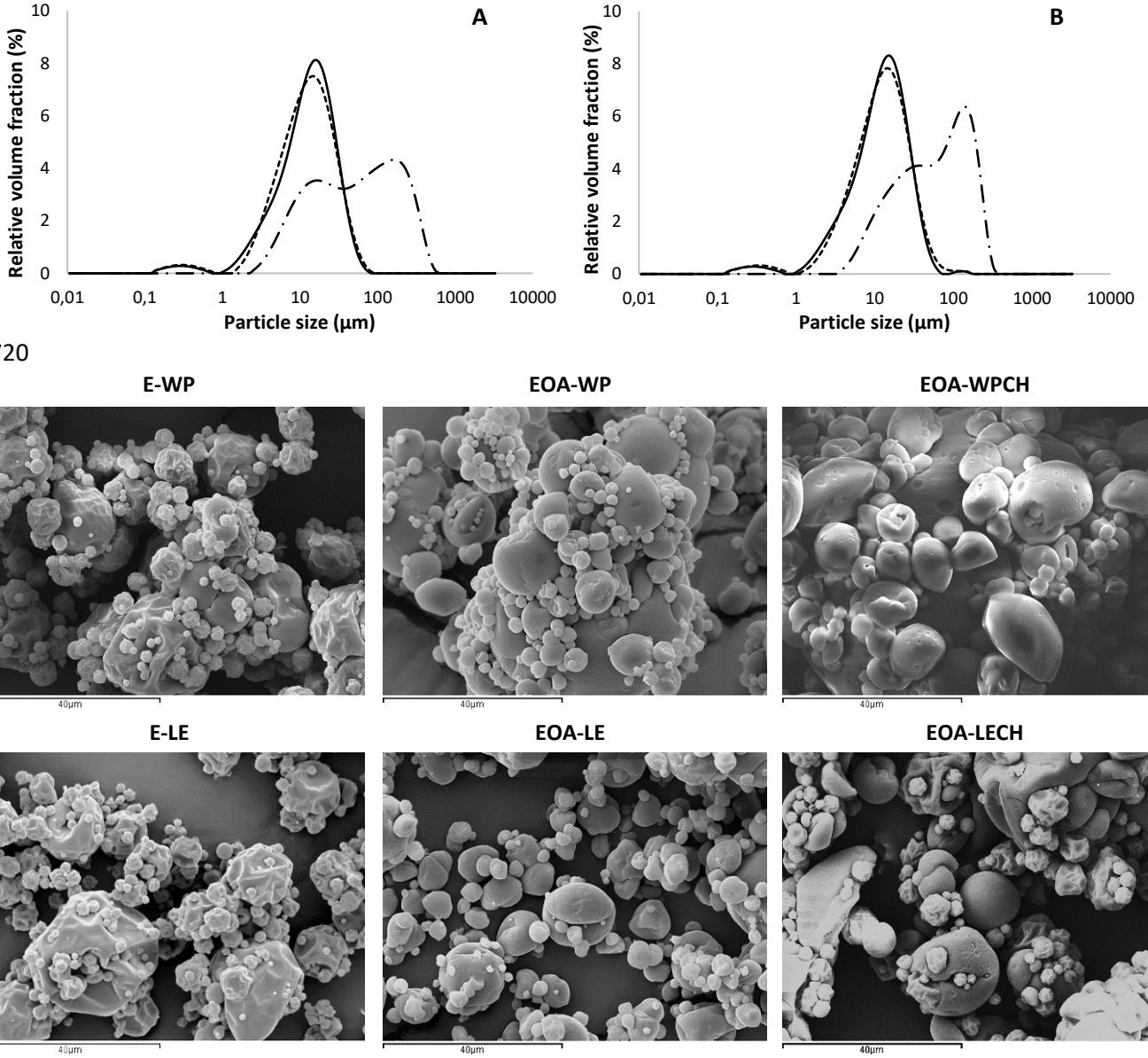

720

721

722 **Figure 2.** Typical particle size distributions of powders prepared using whey protein (A) and lecithin (B)

723 as wall materials, incorporating or not oleic acid and chitosan (—— E; ---- EOA; — · — · EOA-CH). SEM

724 micrographs of the different encapsulated eugenol particles (x1500) are also shown.

725

726

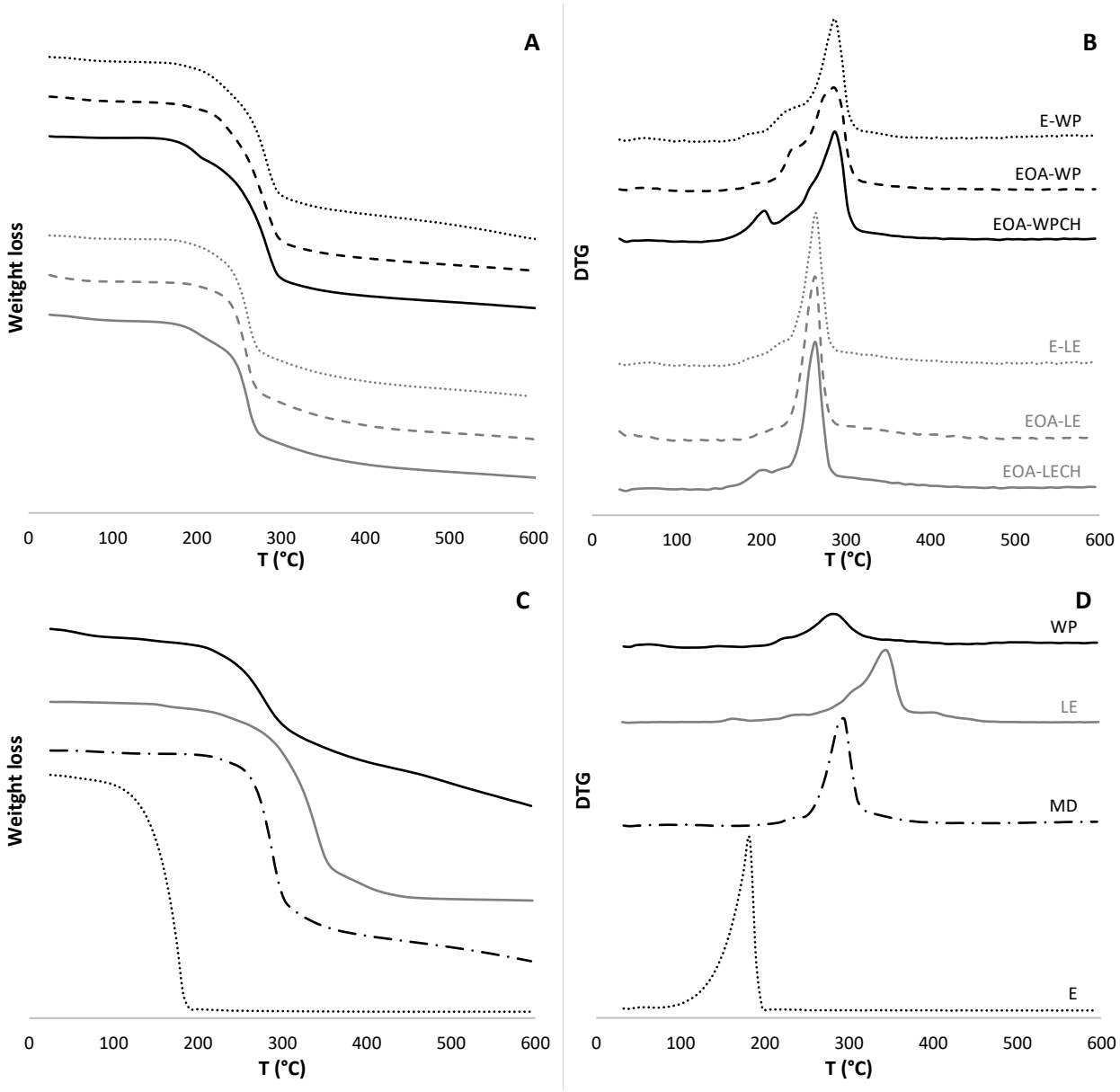

727

728 **Figure 3.** Weight loss curves (A and C) and derivative curves (B and D) from TGA analysis from 25°C to

729 600°C of encapsulated samples (A and B) and different pure components (C and D).

730

731

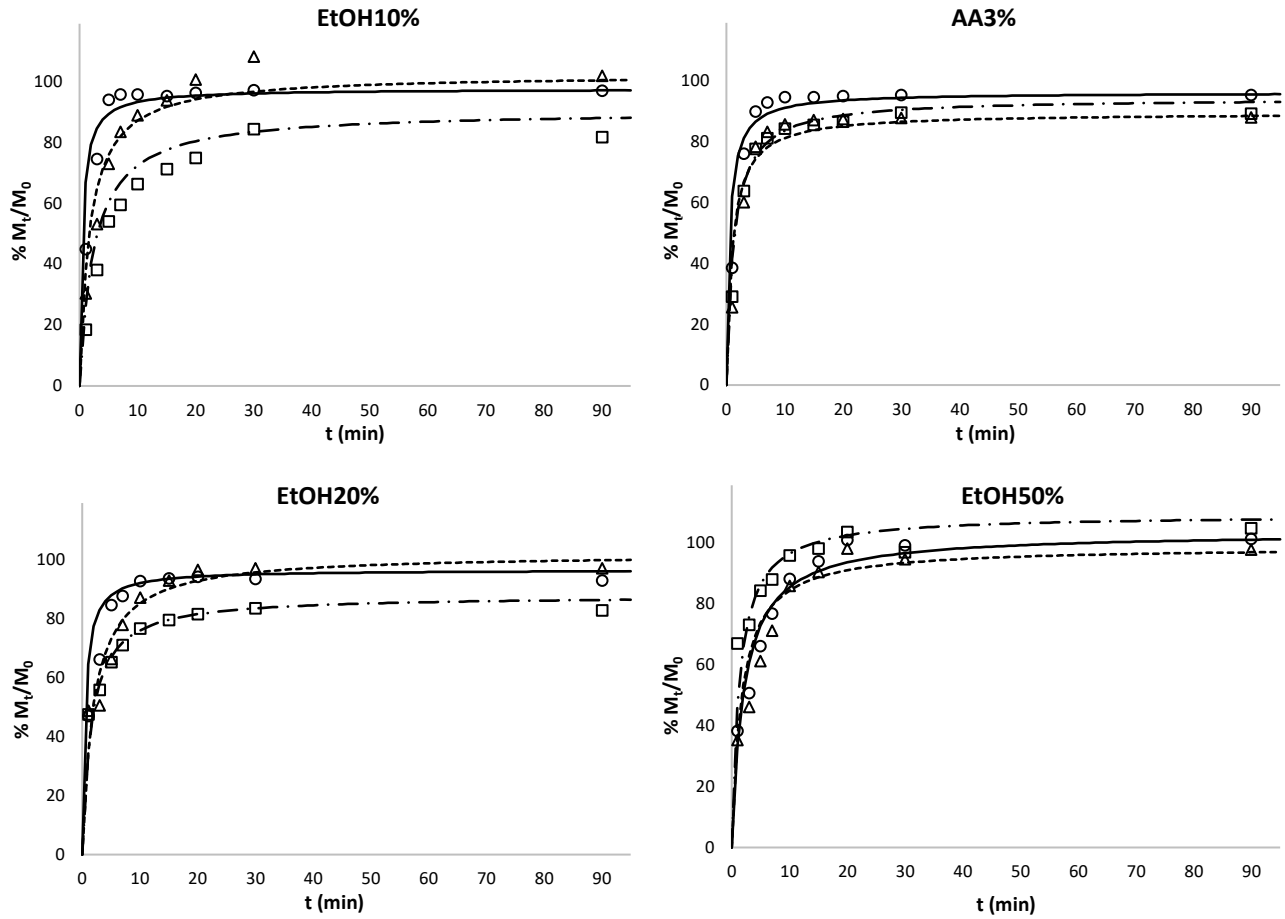

732

733

734 **Figure 4.** Percentage of eugenol released at each time (M_t/M_0) from lecithin-based powders in four
735 different aqueous food simulants: 3% acetic acid, 10% ethanol, 20% ethanol and 50% ethanol.
736 Experimental data (○ E-LE; △ EOA-LE; □ EOA-LECH) and values predicted by Peleg's model (—— E-LE;
737 ---- EOA-LE; — · — · EOA-LECH).

738

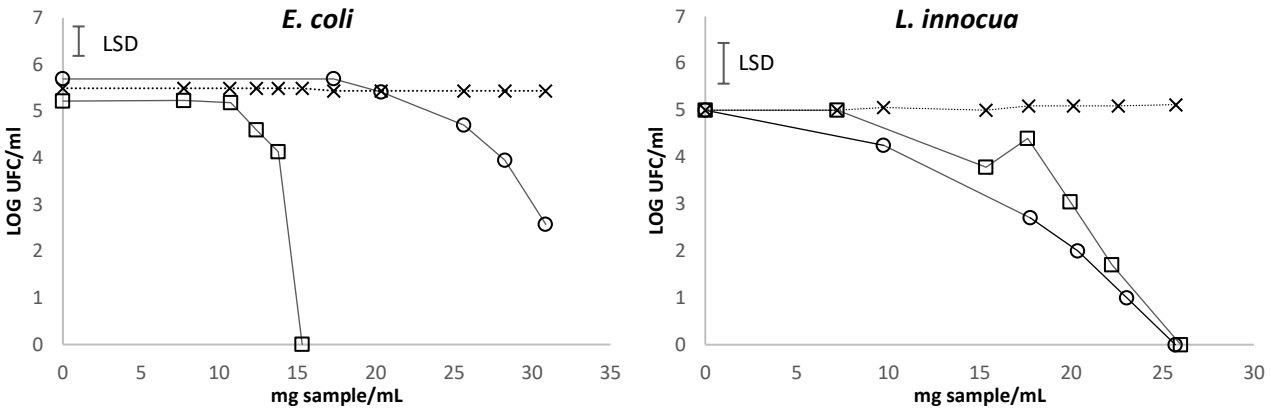

739

740 **Figure 5.** Antimicrobial activity of encapsulated eugenol particles (□ E; ○ EOA; × Control) against

741 *E. coli* and *L. innocua*. Mean values and 95% LSD intervals.

742

743

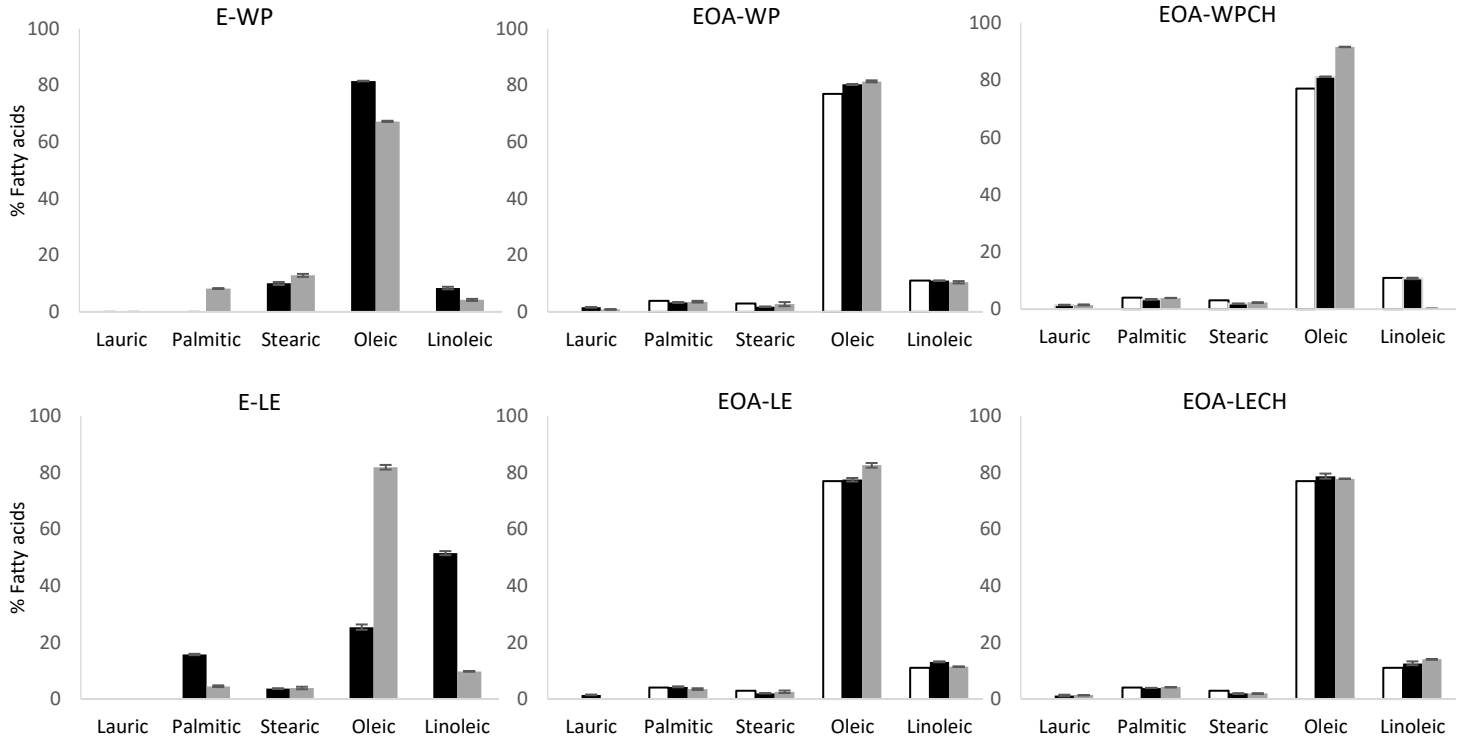

744

745 **Figure S1**. Profile of major fatty acids (individual content with respect to the total content) found in the
746 different sample formulations, in the total extracted lipid fraction (black) and in the lipid extracted from
747 the capsule surface (grey). White bars correspond to the profile of fatty acids in the incorporated oleic
748 acid.

749

750 **Table 1.** Theoretical and extractable eugenol content (mg/g dried powder), encapsulation efficiency and
751 eugenol content on the particle surface (SLC) of different encapsulates. Antioxidant activity in terms of
752 EC_{50} values of particles encapsulating eugenol was also shown referred per mass unit of powder and mass
753 unit of the encapsulated eugenol. Mean values and (standard deviation).

Formulation	Theoretical eugenol (mg/g)	Extractable eugenol (mg/g)	Encapsulation efficiency (%)	Eugenol in SLC(1) (mg/g powder)	% Eugenol in SLC(2)	EC_{50} (mg powder /mg DPPH)	EC_{50} (mg eugenol/ mg DPPH)
E-WP	65.22	62 (2)	95 (3)^{d}	-	-	1.64 (0.05)^{a}	0.107 (0.003)^{a}
EOA-WP	56.60	49 (3)	87 (5)^{c}	2.3 (0.6)^{a}	4.13 (1.14)^{a}	2.12 (0.15)^{a}	0.120 (0.008)^{a}
EOA-WPCH	56.43	12.6 (1.7)	22 (3)^{a}	34.0 (1.4)^{c}	60 (3)^{c}	7.8 (0.9)^{c}	0.44 (0.05)^{c}
E-LE	65.22	64 (4)	98 (6)^{d}	-	-	1.78 (0.14)^{a}	0.116 (0.009)^{a}
EOA-LE	56.60	53 (3)	95 (5)^{d}	1.9 (0.5)^{a}	3.31 (0.02)^{a}	1.709 (0.015)^{a}	0.1114 (0.0010)^{a}
EOA-LECH	56.43	26.2 (1.9)	46 (3)^{b}	28.0 (0.4)^{b}	49.6 (0.08)^{b}	4.6 (0.3)^{b}	0.260 (0.019)^{b}
Pure E							0.092 (0.002)^{a}

754

755 ^{abcd} Different letters in the same column indicate significant differences among formulations ($p<0.05$).

756 (1) Estimated from surface lipid content values (SLC) and nominal E:OA ratio in the powders

757 (2) Percentage of the incorporated eugenol not encapsulated in the samples, deduced from the SLC and
758 E:OA ratio in the powders.

759

760 **Table S1.** Mass fraction of each component (g/g total solids) and % total solids of the different

761 formulations.

Formulation	WP*	LE*	MD*	Eugenol	OA*	CH*	% Total solids
E-WP	0.022	-	0.913	0.065	-	-	43
EOA-WP	0.019	-	0.792	0.057	0.132	-	56
EOA-WPCH	0.019	-	0.790	0.056	0.132	0.003	56.16
E-LE	-	0.022	0.913	0.065	-	-	43
EOA-LE	-	0.019	0.792	0.057	0.132	-	56
EOA-LECH	-	0.019	0.790	0.056	0.132	0.003	56.16

762 * WP: Whey Protein Isolate; LE: Lecithin; MD: Maltodextrin; OA: Oleic acid; CH: Chitosan

763

764 **Table S2.** Zeta potential, pH, rheological parameters and apparent viscosity at 50 s^{-1} of the different

765 emulsions.

Formulation	pH	Z-Potencial (mV)*	Z-Potencial (mV) pH=4	K (Pa·s^n)·100	n	η_{50} (mPa·s)
E-WP	6.6	-28.9 (1.5)^{b}	+19. (0.4)^{a}	5.81 (0.18)^{a}	0.993 (0.004)^{cd}	56.2 (1.9)^{a}
EOA-WP	5.7	-32.5 (0.9)^{a}	+12 (2)^{a}	6.95 (0.15)^{a}	0.995 (0.005)^{d}	68.0 (1.3)^{ab}
EOA-WPCH	4.1	+40 (3)^{c}	+40 (3)^{b}	41.65 (11.13)^{b}	0.836 (0.018)^{b}	219 (46)^{c}
E-LE	4.3	-46.6 (0.5)^{d}	-	73 (0.9)^{a}	0.988 (0.005)^{cd}	69 (8)^{ab}
EOA-LE	4.4	-45.7 (0.5)^{d}	-	90 (10)^{a}	0.982 (0.004)^{c}	84 (9)^{b}
EOA-LECH	4.0	+61.5 (0.9)^{e}	-	69 (17)^{c}	0.726 (0.020)^{a}	214 (11)^{c}

766

767 ^{abcd} Different letters in the same column indicate significant differences among formulations ($p<0.05$).

768 *at the pH of the emulsion

769

Table S3. Moisture content and thermal degradation temperatures (onset values, T_{onset} and value at maximum degradation rate, T_{max}) of the particles using whey protein and lecithin as wall materials, incorporating or not oleic acid and chitosan. Mean values and (standard deviation).

Formulation	% MC (dry weight basis)	T_{max} (°C)	T_{onset} (°C)
E-WP	3.01 (0.02)^{d}	283.7 (0.8)^{c}	221.4 (0.7)^{ab}
EOA-WP	2.74 (0.09)^{c}	282 (2)^{b}	222 (2)^{ab}
EOA-WPCH	1.50 (0.06)^{b}	284.2 (1.0)^{c}	227 (13)^{b}
E-LE	2.84 (0.05)^{c}	259,8 (0,6)^{a}	214.8 (0,9)^{a}
EOA-LE	1.77 (0.03)^{a}	258,6 (0,3)^{a}	224.1 (1.6)^{ab}
EOA-LECH	2.97 (0.14)^{c}	259,4 (0,3)^{a}	226.4 (0.5)^{b}

^{abcd} Different letters in the same column indicate significant differences among formulations ($p<0.05$).

780 **Table S4.** Lipid profile of the different formulations expressed as total (TLC) and superficial lipid content (SLC), in mg fatty acid/g powder. Total fatty acids is the sum of the

781 different lipids in TLC and SLC. % SLC is the total amount of fatty acids present on the surface with respect to the total lipid content. Mean values (and standard deviation).

	E-WP		**EOA-WP**		**EOA-WPCH**		**E-LE**		**EOA-LE**		**EOA-LECH**	
Fatty acids	**TLC**	**SLC**	**TLC**	**SLC**	**TLC**	**SLC**	**TLC**	**SLC**	**TLC**	**SLC**	**TLC**	**SLC**
Lauric C12:0	n.d.*	n.d.	1.95 (0.04)	0.046 (0.014)	1.79 (0.05)	1.18 (0.18)	n.d.	n.d.	1.8 (0.2)	n.d.	1.5 (0.4)	0.869 (0.015)
Miristic C14:0	n.d.	n.d.	0.592 (0.014)	0.013 (0.018)	0.583 (0.095)	0.41 (0.03)	n.d.	n.d.	0.58 (0.05)	n.d.	0.51 (0.08)	0.304 (0.004)
Palmitic C16:0	n.d.	0.0130 (0.0004)	4.03 (0.10)	0.19 (0.04)	4.186 (0.07)	3.096 (0.108)	1.36 (0.12)	0.051 (0.005)	5.4 (0.5)	0.15 (0.03)	4.7 (0.2)	2.71 (0.03)
Margaric C17:0	n.d.	0.0115 (0.0007)	n.d.	0.0099 (0.0002)	n.d.	0.032 (0.002)	n.d.	n.d.	n.d.	n.d.	n.d.	n.d.
Estearic C18:0	0.0386 (0.0007)	0.0202 (0.0004)	2.214 (0.009)	0.1443 (0.0018)	2.290 (0.009)	1.81 (0.04)	0.317 (0.013)	0.044 (0.006)	2.56 (0.09)	0.1117 (0.0008)	2.325 (0.007)	1.251 (0.010)
Oleic C18:1 (n9)	0.31 (0.02)	0.106 (0.002)	97.14 (1.09)	4.4 (1.2)	98.8 (1.3)	73 (3)	2.19 (0.09)	0.927 (0.014)	98 (4)	3.6 (0.6)	95 (3)	50.8 (0.8)
Vaccenic C18:1 (n7)	n.d.	n.d.	0.57 (0.03)	0.031 (0.009)	0.3 (0.5)	0.009 (0.012)	n.d.	n.d.	0.5 (0.4)	n.d.	0.680 (0.017)	0.079 (0.003)
Linoleic C18:2	0.032 (0.004)	0.0067 (0.0007)	13.34 (0.24)	0.57 (0.18)	13.06 (0.14)	0.1171 (0.0004)	4.5 (0.4)	0.111 (0.004)	16.6 (1.0)	0.50 (0.09)	15.2 (1.4)	9.14 (0.16)
Linolenic C18:3	n.d.	n.d.	n.d.	n.d.	n.d.	n.d.	0.32 (0.04)	n.d.	0.28 (0.03)	n.d.	0.24 (0.02)	0.16571 (0.00009)
Arachidic C20:0	n.d.	n.d.	0.258 (0.002)	n.d.	0.12 (0.17)	n.d.	n.d.	n.d.	0.257 (0.013)	n.d.	n.d.	n.d.
Gondoic C20:1	n.d.	n.d.	0.674 (0.010)	n.d.	0.55 (0.03)	n.d.	n.d.	n.d.	0.530 (0.015)	n.d.	0.54 (0.03)	n.d.
Behenic C22:0	n.d.	n.d.	0.108 (0.004)	n.d.	n.d.	n.d.	n.d.	n.d.	n.d.	n.d.	n.d.	n.d.
Lignoceric C24:0	n.d.	n.d.	0.0917 (0.0010)	n.d.	n.d.	n.d.	n.d.	n.d.	n.d.	n.d.	n.d.	n.d.
Total fatty acids (mg/g)	**0.38 (0.03)**	**0.157 (0.003)**	**121.0 (1.5)**	**5.5 (1.5)**	**121.7 (1.5)**	**79 (3)**	**8.6 (0.7)**	**1.13 (0.03)**	**127 (6)**	**4.4 (0.7)**	**121 (5)**	**65.36 (1.05)**
% SLC	**40.85**		**4.51**		**65.10**		**13.11**		**3.45**		**54.08**	

782 * n.d.: Non-detected.

Table S5. Maximum eugenol release ratio (M_∞/M_0)* and parameters of Peleg´s model for the different encapsulated systems in the different food simulants: inverse of the initial release rate (k_1) (min/(mg eugenol /g powder)) and equilibrium value, M_∞ ($1/k_2$) (mg eugenol/g powder).

Formulation	Parameters	SIMULANTS			
		Ethanol 10%	**Ethanol 20%**	**Ethanol 50%**	**AA 3%**
E-WP	k_1	0.0065 (0.0009)^{a,1}	0.0053 (0.0010)^{a,1}	0.039 (0.009)^{a,1}	0.0041 (0.0019)^{a,1}
	$M_\infty=1/k_2$	60.3 (0.3)^{d,1}	60.2 (0.8)^{d,1}	68.5 (1.7)^{d,2}	60.22 (1.06)^{d,1}
	M_∞/M_0 (%)	97.1 (1.7)^{c,1}	97.1 (1.3)^{c,1}	100 (0)^{a,1}	97.1 (1.7)^{bcd,1}
	R^2	≥ 0.999	≥ 0.999	≥ 0.999	≥ 0.999
EOA-WP	k_1	0.0109 (0.0013)^{a,1}	0.012870^{a,1}	0.02888 (0.00102)^{a,1}	0.018 (0.013)^{ab,1}
	$M_\infty=1/k_2$	47.4 (0.7)^{c,1}	48.78 (0.15)^{c,1}	56.6 (4.4)^{c,2}	59 (5.3)^{c,2}
	M_∞/M_0 (%)	89.4 (1.3)^{b,1}	92.0 (0.3)^{b,1}	100 (0)^{a,2}	100 (0)^{c,2}
	R^2	≥ 0.998	≥ 0.998	≥ 0.999	≥ 0.998
EOA-WPCH	k_1	0.06 (0.03)^{bc,1}	0.09 (0.02)^{bc,1}	0.159 (0.006)^{b,2}	0.09 (0.03)^{c,1}
	$M_\infty=1/k_2$	10.38 (0.02)^{a,1}	14.5 (0.3)^{a,12}	18.6 (1.8)^{a,2}	16.7 (0.3)^{a,2}
	M_∞/M_0 (%)	74.16 (0.14)^{a,1}	100 (0)^{c,2}	100 (0)^{a,2}	100 (0)^{cd,2}
	R^2	≥ 0.958	≥ 0.945	≥ 0.925	≥ 0.998
E-LE	k_1	0.007 (0.005)^{a,1}	0.0080 (0.0013)^{a,1}	0.032 (0.008)^{a,1}	0.009 (0.003)^{a,1}
	$M_\infty=1/k_2$	62.6 (3.1)^{d,12}	61.7 (1.4)^{d,12}	66.7 (6.8)^{d,2}	58.6 (0.8)^{d,1}
	M_∞/M_0 (%)	99.2 (1.4)^{c,1}	97.8 (0.3)^{c,1}	98,9 (2.0)^{a,1}	96.1 (1.3)^{bc,1}
	R^2	≥ 0.999	≥ 0.998	≥ 0.997	≥ 0.998
EOA-LE	k_1	0.030 (0.002)^{ab,1}	0.032 (0.008)^{ab,1}	0.03 (0.03)^{a,1}	0.020 (0.006)^{ab,1}
	$M_\infty=1/k_2$	58.4 (0.7)^{d,2}	56.7 (0.6)^{d,2}	56.5 (4.6)^{c,2}	51 (0.7)^{c,1}
	M_∞/M_0 (%)	100 (0)^{c,2}	99.4 (0.9)^{c,2}	97 (5)^{a,2}	89.4 (1.2)^{a,1}
	R^2	≥ 0.997	≥ 0.993	≥ 0.958	≥ 0.996
EOA-LECH	k_1	0.095 (0.008)^{c,1}	0.061 (0.014)^{c,1}	0.042 (0.013)^{a,1}	0.047 (0.011)^{b,1}
	$M_\infty=1/k_2$	26.3 (2.3)^{b,1}	25.4 (0.8)^{b,1}	31.8 (2.4)^{b,2}	27.4 (1.3)^{b,12}
	M_∞/M_0 (%)	91 (8)^{b,12}	88 (3)^{a,1}	100 (0)^{a,3}	94.4 (4.4)^{b,2}
	R^2	≥ 0.986	≥ 0.999	≥ 0.997	≥ 0.994

* related to the initial eugenol amount determined by methanol extraction.

^{abcd} Different letters in the same column indicate significant differences among formulations ($p<0.05$).

^{1234} Different numbers in the same line indicate significant differences among food simulants ($p<0.05$).